Molecular Therapy
Oncolytics
Original Article

Knockdown of SENP1 inhibits HIF-1α SUMOylation and suppresses oncogenic CCNE1 in Wilms tumor

Shibo Zhu,[1] Jinhua Hu,[1] Yanhong Cui,[1] Shen Liang,[1] Xiaofeng Gao,[1] Jin Zhang,[1] and Wei Jia[1]

[1]Department of Pediatric Urology, Guangzhou Women and Children's Medical Center, Guangzhou Medical University, No. 9, Jinsui Road, Guangzhou 510623, Guangdong Province, China

Based on our initial bioinformatics finding of the upregulated expression of sentrin-specific protease 1 (SENP1) and cyclin E1 (CCNE1) in Wilms tumor, this study aimed to illustrate the molecular mechanism of SENP1 in Wilms tumor, which involved the hypoxia-inducible factor 1α (HIF-1α)/stanniocalcin-1 (STC1)/CCNE1 axis. Wilms tumor and adjacent normal tissues were clinically collected. Gain- and loss-of-function assays were performed to evaluate the effects of the regulatory axis on malignant phenotypes of Wilms tumor cells. A mouse model of Wilms tumor xenografts was further established for *in vivo* substantiation. Overexpression of CCNE1 and SENP1 occurred in Wilms tumor tissues and cells. Silencing SENP1 inhibited viability and enhanced cell-cycle arrest of Wilms tumor cells. SENP1 promoted STC1 expression and upregulated CCNE1 by driving the small ubiquitin-like modifier (SUMO) ylation of HIF-1α, which ultimately promoted the malignant phenotypes of Wilms tumor cells. It was further confirmed that silencing SENP1 downregulated the expression of CCNE1 and restricted tumorigenicity of Wilms tumor cells *in vivo*. Taken together, SENP1 elevated STC1 expression by driving the SUMOylation of HIF-1α, thereby upregulating the expression of CCNE1 and ultimately promoting the development of Wilms tumor.

INTRODUCTION

Wilms tumor is a frequently occurring embryonal tumor in children and can also occur in adults in rare cases.[1] Wilms tumor is featured with abdominal pathology along with few constitutional symptoms, although hematuria rarely can be a presenting characteristic.[2] The recommended treatment strategies for Wilms tumor include primary surgery and neoadjuvant chemotherapy, which can be initiated for typical patients with Wilms tumor in the absence of histological confirmation.[3] However, poor prognosis and increased relapse rates still exist in some subgroups of Wilms cancer, and about one in ten children with Wilms tumor dies of this disease despite modern treatment approaches.[4,5] In this sense, the development of Wilms tumor treatment is in urgent need of investigations on novel biomarkers involved in the pathogenesis of Wilms tumor.

Sentrin-specific protease 1 (SENP1) is regarded as a model for the ubiquitin-specific protease family and accountable for processing small ubiquitin-like modifier (SUMO).[6] Aberrant regulation of SENP1 was unfolded in a variety of cancers, such as breast cancer,[7] pancreatic cancer,[8] and hepatocellular carcinoma,[9] and has thus been suggested to be an oncogene,[10] whereas the potential participation of SENP1 in Wilms tumor remains to be established. Of note, SENP1 is able to increase the expression of hypoxia-inducible factor 1α (HIF-1α) in ovarian cancer cells under hypoxia.[11] HIF-1α is an important regulator of the tumor cell response to hypoxia, which can orchestrate mechanisms implicated in cancer aggressiveness as well as metastatic behavior.[12] HIF-1α, as one of the components of the COX-2 ((cyclooxygenase-2−ΔΔCT; CT, threshold cycle; ΔΔCT = CT([target gene] − CT[control gene])experimental group − CT([target gene] − CT[control gene])control group) pathway, was found to be increased in mouse and human tumor tissues in Wilms tumor.[13] Intriguingly, it was previously reported that HIF-1α was upregulated in Wilms tumor.[14] Importantly, it was found that HIF-1α could positively regulate the expression of stanniocalcin-1 (STC1) in clear cell renal cell carcinoma.[15] STC1 is identified as a secreted glycoprotein that is involved in different biological activities, such as angiogenesis and inflammation.[16] Cyclin E1 (CCNE1) is considered to be a positive mediator of the cell cycle controlling the G1-S-phase transition of cervical cancer cells.[17] Notably, CCNE1, as a oncogene, was regulated by WW domain-containing oxidoreductase (WWOX) in the carcinogenesis of Wilms tumor.[18]

With the consideration of all of the above findings, we propose a hypothesis in the current study that SENP1 may affect Wilms tumor development through the regulation of the HIF-1α/STC1/CCNE1 axis. Herein, a mechanism involving the SENP1-mediated HIF-1α/STC1/CCNE1 axis was identified to affect the malignant phenotypes of Wilms tumor. In this study, we demonstrated that SENP1 upregulated STC1 expression by augmenting HIF-1α SUMOylation, thereby upregulating oncogenic CCNE1 and ultimately accelerating Wilms tumor progression.

Received 8 February 2021; accepted 14 July 2021;
https://doi.org/10.1016/j.omto.2021.07.007.

Correspondence: Shibo Zhu, Department of Pediatric Urology, Guangzhou Women and Children's Medical Center, Guangzhou Medical University, No. 9, Jinsui Road, Guangzhou 510623, Guangdong Province, China.
E-mail: docorzhushibo@163.com
Correspondence: Wei Jia, Department of Pediatric Urology, Guangzhou Women and Children's Medical Center, Guangzhou Medical University, No. 9, Jinsui Road, Guangzhou 510623, Guangdong Province, China.
E-mail: jiawei198044@hotmail.com

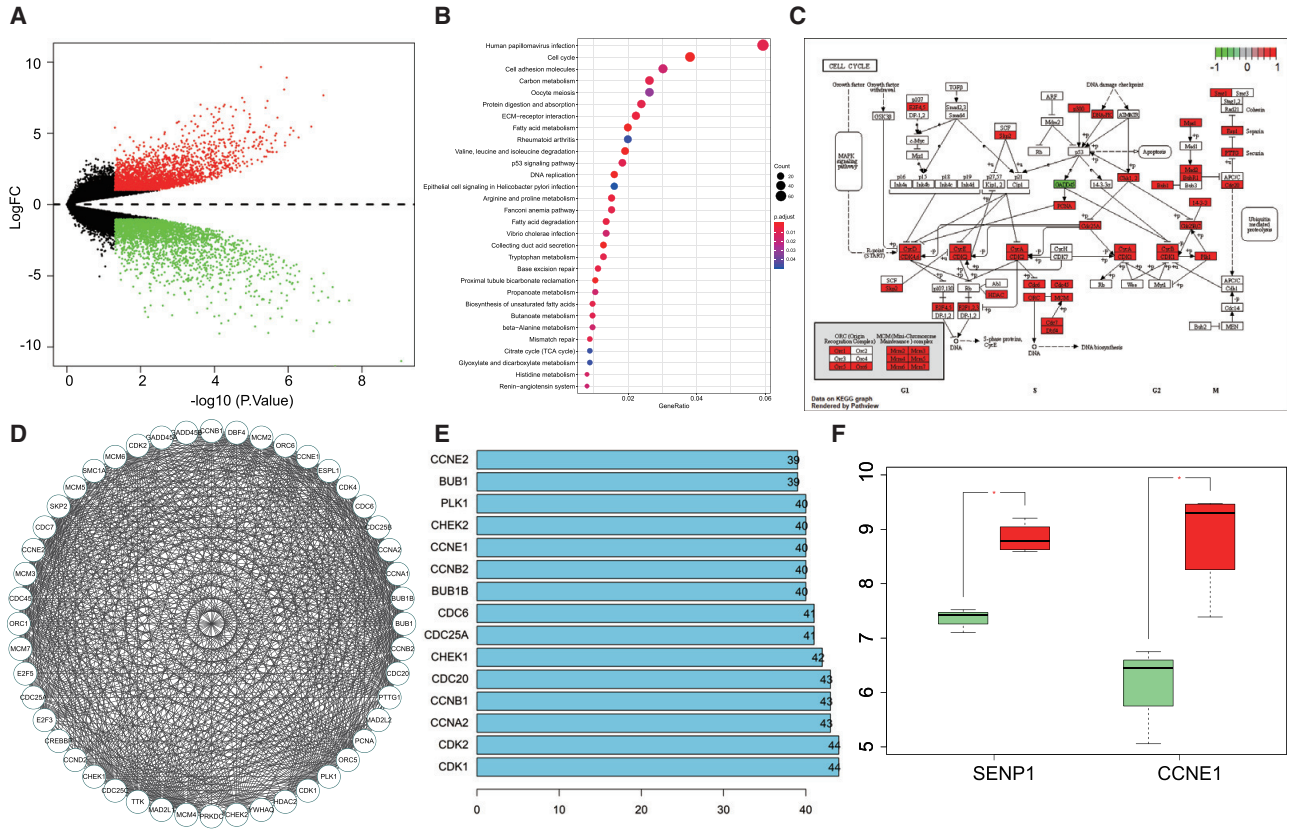

Figure 1. SENP1 may affect the cell-cycle signaling pathway of Wilms tumor by regulating the expression of CCNE1

(A) The volcanic map of differential genes in GSE11151. The x axis represents −log10(p value), the y axis represents logFC (log fold change), the red dots represent the gene with appreciably high expression in tumor tissue, and the green dots represent the gene with appreciably low expression. (B) KEGG pathway enrichment analysis of differential genes. The abscissa represents GeneRatio, the ordinate represents KEGG entry, and the circle size in the map represents the number of differentially expressed genes enriched in this entry. The color represents the p value of enrichment, and the histogram on the right is the color scale. (C) Differentially expressed genes in the cell-cycle signaling pathway are labeled; red represents high expression genes, and green represents low expression genes. (D) Differential gene interaction analysis in the cell-cycle signaling pathway; each circle represents a gene, and the lines between circles indicate the existence of an interaction relationship. If the gene has more interaction genes, the degree value and the core degree are higher. (E) The statistics for the core degree of different genes in the cell cycle in the interaction network diagram (the x axis represents the degree value, and the y axis represents the gene name). (F) The differential expression of candidate genes SENP1 and CCNE1 in GSE11151 (the x axis represents the gene name, and the y axis represents the expression level); the green box graph represents the normal sample, and the red box graph represents the tumor samples (*FDR < 0.05).

RESULTS

SENP1 might affect the cell-cycle signaling pathway of Wilms tumor by regulating the expression of CCNE1

The expression microarray GSE11151 of Wilms tumor obtained from the Gene Expression Omnibus (GEO) database was used for differential analysis, which revealed that 3,254 differentially expressed genes (DEGs) were obtained (Figure 1A). Then, enrichment analysis of the Kyoto Encyclopedia of Genes and Genomes (KEGG) pathway showed that these DEGs were mainly enriched in cell-cycle-related signaling pathways (Figure 1B), suggesting that the abnormality of the cell-cycle signaling pathway may affect the development of Wilms tumor. Further labeling of these DEGs in the cell-cycle signaling pathway using map04110 (https://www.kegg.jp/dbget-bin/www_bget?map04110) showed that most of them were highly expressed in Wilms tumor (Figure 1C).

Then, we analyzed the interaction of the DEGs in the cell-cycle signaling pathway through the STRING database, constructed the gene-gene interaction network diagram (Figure 1D), and counted the degree value of the core genes (Figure 1E). The results showed that the core degree value of 13 genes was greater than 40, suggesting that they may be more critical in the regulation of cell cycle. Among these 13 genes, we found CCNE1 as one of the core genes. In GSE11151, we found that SENP1 and CCNE1 were highly expressed (Figure 1F). These results suggest that SENP1 may affect the cell-cycle signaling pathway of Wilms tumor by regulating the expression of CCNE1.

SENP1 was highly expressed in the tissues and cells of Wilms tumor and was associated with poor prognosis

A previous study has shown that CCNE1 acts as a cyclin,[18] but its upstream regulation mechanism is still unknown. We determined

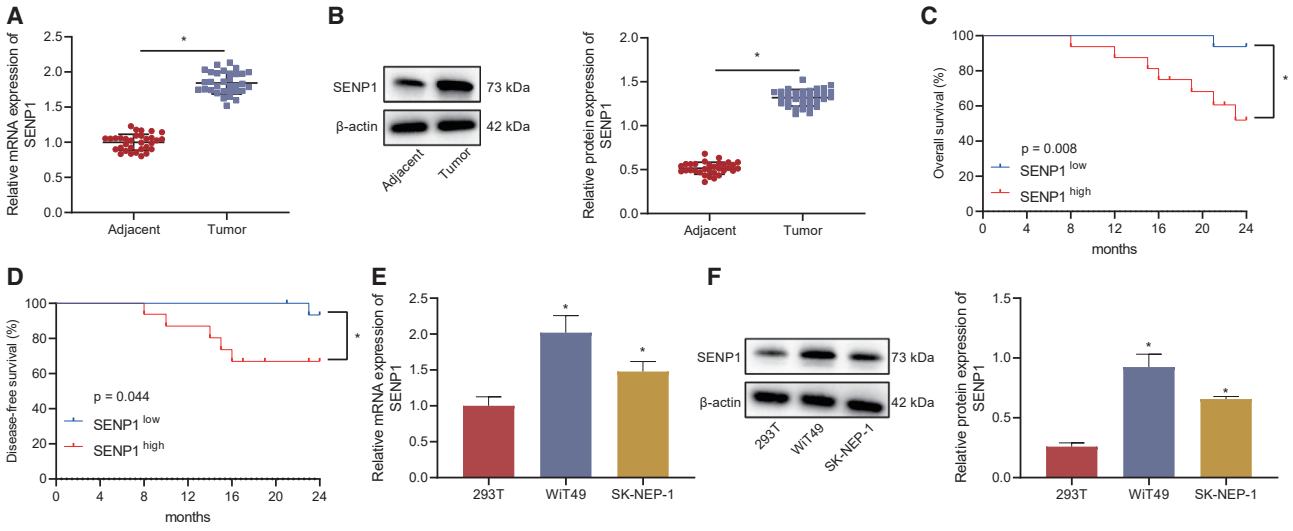

Figure 2. SENP1 is highly expressed in the tissues and cells of Wilms tumor and is associated with poor prognosis

(A) qRT-PCR was used to detect the mRNA expression of SENP1 in Wilms tumor tissues. Adjacent = 32; tumor = 32. *p < 0.05 versus adjacent tissue. (B) Western blot was used to detect the protein expression of SENP1 in Wilms tumor tissues. Adjacent = 32; tumor = 32. *p < 0.05 versus adjacent tissue. (C and D) The correlation between SENP1 expression and OS and DFS by the Kaplan-Meier method. (E) mRNA expression of SENP1 in Wilms tumor cells WiT49, SK-NEP-1, and normal renal cells 293T by qRT-PCR. *p < 0.05 versus 293T cell. (F) The protein expression of SENP1 in Wilms tumor cells WiT49 and SK-NEP-1 and normal renal tissue cells 293T was assayed by western blot. *p < 0.05 versus 293T cell.

SENP1 mRNA and protein expression in Wilms tumor tissues and paracancerous tissues. The results showed that the expression of SENP1 in Wilms tumor tissues was appreciably higher than that in paracancerous tissues (Figures 2A and 2B). Patients with Wilms tumor (n = 32) were divided into the SENP1 high expression group and low expression group according to the median value of SENP1 expression level. Kaplan-Meier results showed that overall survival (OS) and disease-free survival (DFS) of patients with high SENP1 expression were appreciably lower than those of patients with low SENP1 expression, suggesting that high SENP1 expression is associated with poor prognosis (Figures 2C and 2D).

We further determined the expression of SENP1 in Wilms tumor cell lines by quantitative reverse transcriptase polymerase chain reaction (qRT-PCR) and western blot analysis. The results showed that compared with 293T cells, SENP1 expression in Wilms tumor cells WiT49 and SK-NEP-1 was appreciably increased, and SENP1 expression in WiT49 cell lines was higher than that in SK-NEP-1 cells (Figures 2E and 2F). These results indicate that SENP1 is highly expressed in both tissues and cells of Wilms tumor and is associated with poor prognosis.

Silencing of SENP1 inhibited the viability of Wilms tumor cells and promoted cell-cycle arrest

We further investigated the effect of SENP1 gene silencing and overexpression on viability and cell-cycle arrest of Wilms tumor cells. As assayed by qRT-PCR, compared with short hairpin RNA (shRNA) negative control (sh-NC) treatment, the expression of SENP1 in the presence of shRNA targeting SENP (sh-SENP)1-1, sh-SENP1-2, or sh-SENP1-3 was appreciably diminished, and the expression of SENP1 in the sh-SENP1-2 group was the lowest (Figure 3A). So the sh-SENP1-2 sequence was applied to knock SENP1 down for subsequent experiments. Then, in SK-NEP-1 cells, it was found that the expression of SENP1 in response to overexpression plasmid (oe)-SENP1 was appreciably elevated (Figure 3B).

The Cell Counting Kit 8 (CCK-8) assay and Transwell assay results showed that sh-SENP1 transduction appreciably diminished the viability and invasion of WiT49 cells. The transduction of oe-SENP1 had appreciably increased viability and invasion of SK-NEP-1 cells (Figures 3C and 3D). Western blot assay indicated that the expression of Ki67 and proliferating cell nuclear antigen (PCNA) in response to sh-SENP1 was diminished in WiT49 cells, whereas the expression of Ki67 and PCNA in response to oe-SENP1 was increased in SK-NEP-1 cells (Figure 3E).

Flow cytometry showed that in WiT49 cells, G0/G1 cell-cycle arrest was appreciably increased in response to sh-SENP1; G0/G1 cell-cycle arrest of SK-NEP-1 cells was appreciably diminished in response to oe-SENP1 (Figure 3F). These results suggest that silencing SENP1 diminished the viability, invasion, and cell-cycle entry of Wilms tumor cells.

CCNE1 was highly expressed in Wilms tumor tissues and cells

qRT-PCR and western blot results showed that the expression of CCNE1 in Wilms tumor tissues was appreciably higher than that in paracancerous tissues (Figures 4A and 4B). In order to study the correlation between SENP1 and CCNE1 in Wilms tumor

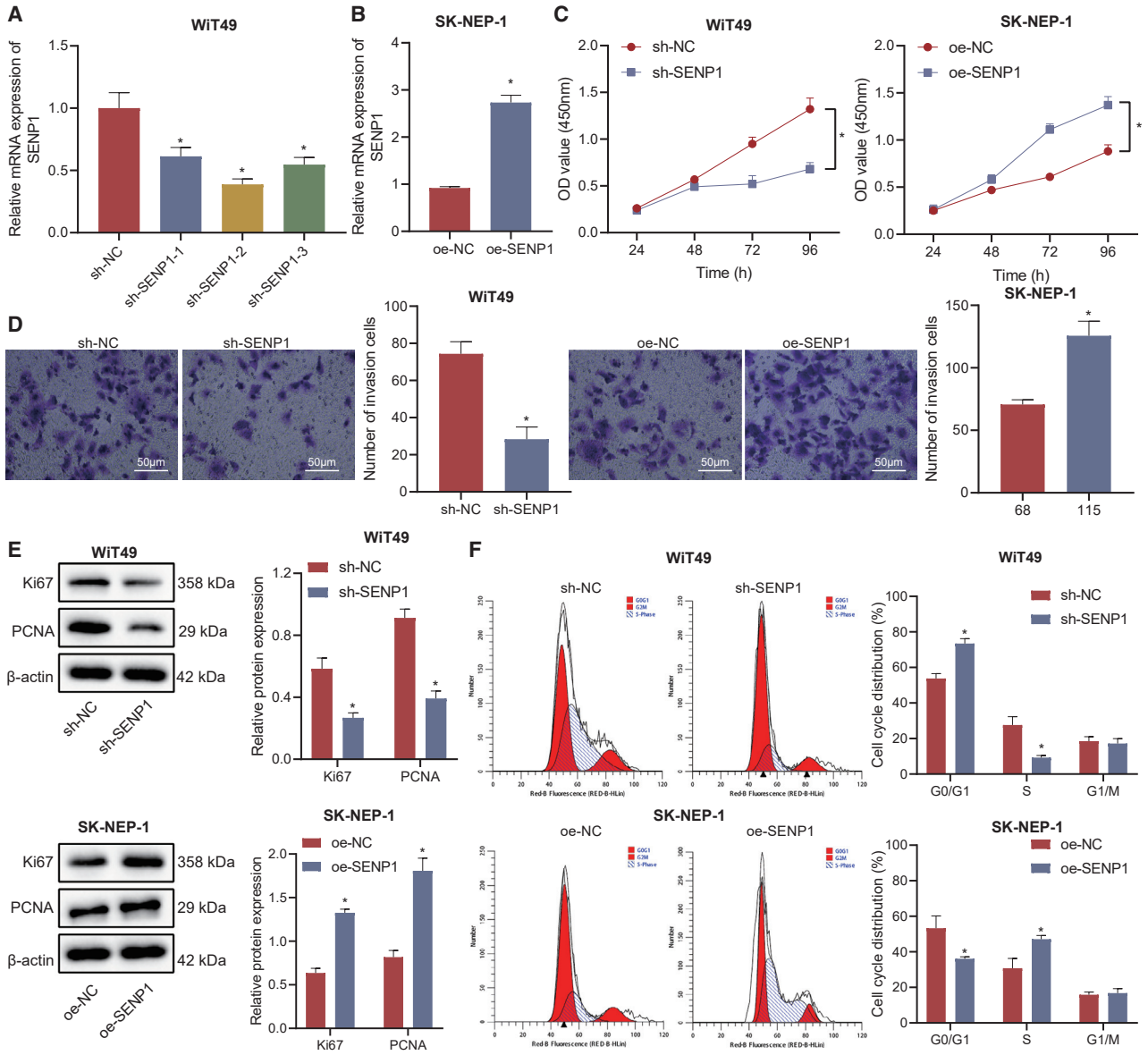

Figure 3. Silencing of SENP1 inhibits the viability of Wilms tumor cells and promotes cell-cycle arrest

(A) qRT-PCR was used to detect the expression of SENP1 in WiT49 cells after silencing SENP1. (B) qRT-PCR was used to detect the expression of SENP1 in SK-NEP-1 cells after overexpression of SENP1. (C) CCK-8 assay was used to detect the viability of WiT49 and SK-NEP-1 cells. (D) Transwell assay was used to detect the invasion of WiT49 and SK-NEP-1 cells. (E) Western blot was used to detect the protein expression of Ki67 and PCNA in WiT49 and SK-NEP-1 cells. (F) Cell cycle of WiT49 and SK-NEP-1 cells was assayed by flow cytometry. *$p < 0.05$ versus the sh-NC group or oe-NC group.

samples, we analyzed the correlation between SENP1 and CCNE1 mRNA expression and found a positive correlation between them (Figure 4C). Kaplan-Meier analysis showed that OS and DFS of patients with high CCNE1 expression were appreciably lower than those of patients with low CCNE1 expression, suggesting that high CCNE1 expression is associated with poor prognosis (Figures 4D and 4E). Further detection of CCNE1 expression in Wilms tumor cells and normal renal cells showed that the expression of CCNE1 in Wilms tumor cells WiT49 and SK-NEP-1 was appreciably higher than that in normal renal cells 293T (Figure 4F). These results demonstrated that CCNE1 is highly expressed in Wilms tumor tissues and cells.

SENP1 promoted viability and cell-cycle progression of Wilms tumor cells by upregulating CCNE1 expression

In order to study the effect of SENP1 on CCNE1 gene expression, western blot analysis was used to detect the expression of CCNE1 in cells after silencing or overexpression of SENP1. The results showed that

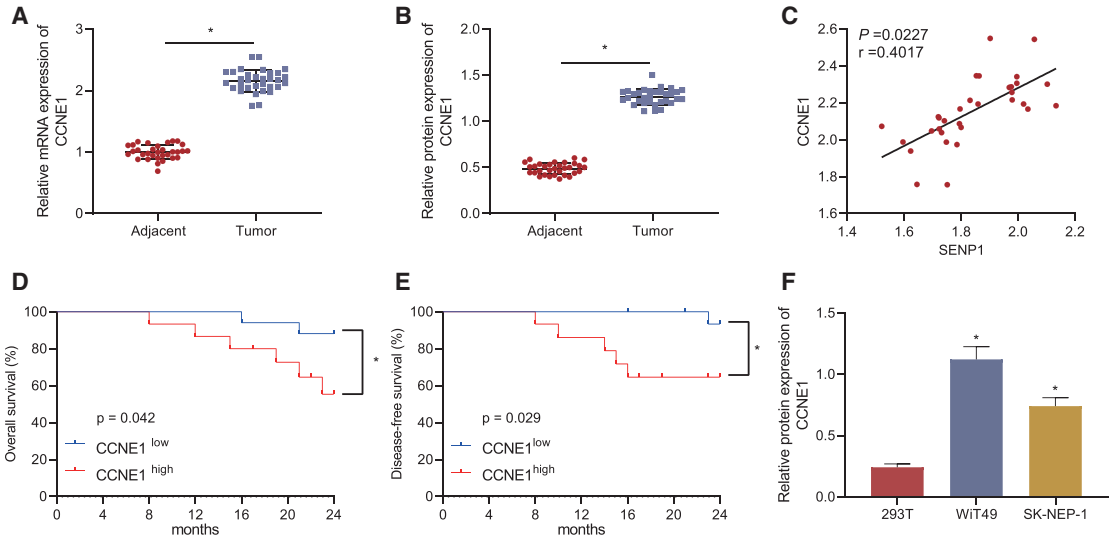

Figure 4. CCNE1 is highly expressed in Wilms tumor tissues and cells

(A) qRT-PCR was used to detect the mRNA expression of CCNE1 in Wilms tumor tissues and adjacent tissues. Adjacent = 32; tumor = 32. *p < 0.05 versus adjacent tissue. (B) Western blot was used to detect the protein expression of CCNE1 in Wilms tumor tissues and adjacent tissues. Adjacent = 32; tumor = 32. *p < 0.05 versus adjacent tissue. (C) Correlation analysis of SENP1 and CCNE1 mRNA expression. (D and E) Correlation analysis of CCNE1 expression with OS and DFS by the Kaplan-Meier method. (F) Western blot detection of CCNE1 protein expression in Wilms tumor cells WiT49, SK-NEP-1, and normal renal tissue cells 293T. *p < 0.05 versus 293T cell.

in WiT49 and SK-NEP-1 cells, the expression of CCNE1 in response to sh-SENP1 was appreciably lowered (Figures 5A and S1A); in WiT49 and SK-NEP-1 cells, the expression of CCNE1 in response to oe-SENP1 was appreciably elevated (Figures 5B and S1B). qRT-PCR was used to detect the expression of CCNE1 in WiT49 cells after silencing and overexpression of CCNE1. The results revealed that compared with sh-NC treatment, the expression of CCNE1 in presence of shRNA targeting CCNE (sh-CCNE)1-1, sh-CCNE1-2, or sh-CCNE1-3 was appreciably diminished, and the expression of CCNE1 in presence of sh-CCNE1-1 was the lowest, so the sequence of sh-CCNE1-1 was used to knock CCNE1 down for subsequent experiments. Further, the expression of CCNE1 in response to oe-CCNE1 was appreciably increased (Figures 5C and S1C).

We further overexpressed CCNE1 on the basis of SENP1 knockdown. The CCK-8 assay and Transwell assay results showed that the viability and invasion in response to sh-CCNE1 were appreciably diminished; compared with sh-SENP1 alone, the viability and invasion in response to sh-SENP1 + oe-CCNE1 were appreciably increased (Figures 5D, 5E, S1D, and S1E). A western blot assay suggested that the expression of Ki67 and PCNA in response to sh-CCNE1 was appreciably diminished; compared with sh-SENP1 alone, the expression of Ki67 and PCNA in response to sh-SENP1 + oe-CCNE1 was appreciably increased (Figures 5F and S1F). Flow cytometric results showed that G0/G1 cell-cycle arrest in response to sh-CCNE1 was appreciably increased; compared with sh-SENP1 alone, G0/G1 cell-cycle arrest in response to sh-SENP1 + oe-CCNE1 was appreciably diminished (Figures 5G and S1G). These results suggest that SENP1 promotes the viability and cell-cycle progression of Wilms tumor cells through upregulation of CCNE1 expression.

SENP1 promoted viability and cell-cycle progression of Wilms tumor cells by activating the HIF-1α/STC1/CCNE1 axis

STC1 is a glycoprotein hormone involved in calcium/phosphate homeostasis, which can regulate various cellular processes during normal development and tumorigenesis. We had previously confirmed that SENP1 can upregulate CCNE1 expression. Therefore, here, we further explored whether SENP1 affects the expression of CCNE1 through regulating STC1 and then affects the viability and cell cycle of Wilms tumor cells. Western blot analysis showed that overexpression of STC1 could partially restore the inhibition of CCNE1 expression induced by SENP1 knockdown, whereas knockdown of STC1 could partially restore the increase of CCNE1 expression induced by SENP1 knockdown (Figures 6A and 6B). These results suggest that overexpression of SENP1 elevated the expression of CCNE1 by upregulating STC1.

Therefore, we speculate that SENP1 may promote the expression of STC1 by driving SUMOylation of HIF-1α. Western blot results showed that the sh-SENP1 transduction had appreciably diminished expression of HIF-1α and p300, whereas the oe-SENP1 transduction displayed notably increased expression of HIF-1α and p300 (Figure 6C).

The results of qRT-PCR showed that compared with sh-NC treatment, the expression of HIF-1α in the presence of shRNA targeting of HIF-1α (sh-HIF-1α)-1, sh-HIF-1α-2, or sh-HIF-1α-3 was appreciably diminished, and the expression of CCNE1 in the sh-HIF-1α-1 group was the lowest. After overexpression of HIF-1α, the expression of CCNE1 in response to oe-HIF-1α was appreciably elevated (Figure 6D). In order to study the relationship among SENP1, HIF-1α, and STC1 expression, we inhibited SENP1 expression and overexpressed HIF-1α in WiT49 cells. The results showed that overexpression of HIF-1α

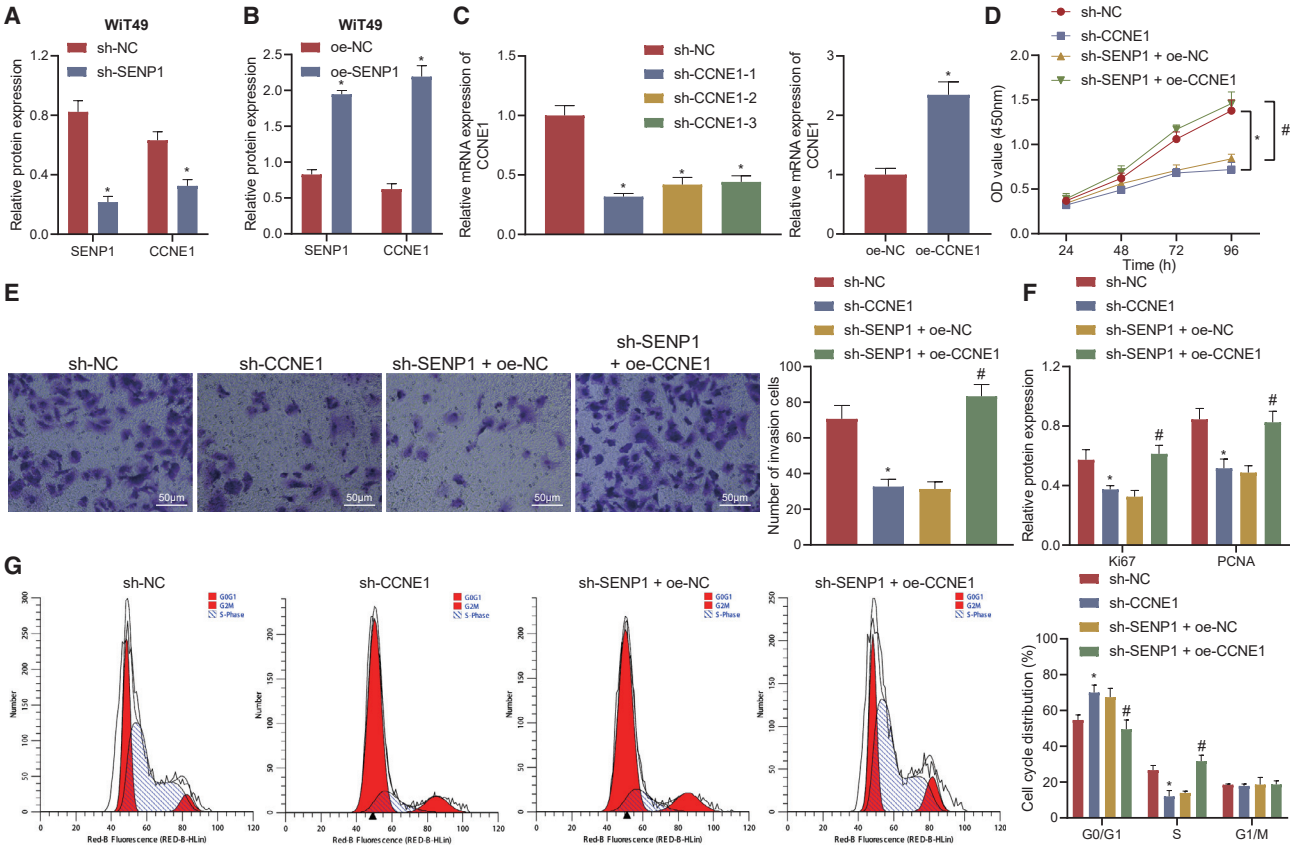

Figure 5. SENP1 promotes viability and cell-cycle progression of Wilms tumor cells by upregulating CCNE1 expression

(A) Western blot was used to detect the expression of CCNE1 in WiT49 cells after SENP1 silencing. (B) Western blot was used to detect the expression of CCNE1 in WiT49 cells after SENP1 overexpression. (C) qRT-PCR was used to detect the expression of CCNE1 in WiT49 cells after SENP1 silencing or overexpression. (D) The CCK-8 assay was used to detect the viability of WiT49 cells in each group. (E) The Transwell assay was used to detect the invasion of WiT49 cells in each group. (F) Western blot was used to detect the protein expression of Ki67 and PCNA in WiT49 cells. (G) Cell-cycle distribution of WiT49 cells was assayed by flow cytometry. *$p < 0.05$ versus sh-NC or oe-NC; #$p < 0.05$ versus sh-SENP1 + oe-NC.

partially restored the inhibition of STC1 expression induced by SENP1 knockdown (Figure 6E). An immunoprecipitation (IP) assay showed that overexpression of SENP1 augmented the deSUMOylation of HIF-1α (Figure 6F). These results indicate that SENP1 promotes STC1 expression by driving SUMOylation of HIF-1α.

The results showed that compared with sh-SENP1 alone, sh-SENP1 + oe-STC1 or sh-SENP1 + oe-HIF-1α had appreciably increased cell viability and invasion, increased Ki67 and PCNA expression, and diminished G0/G1 cell-cycle arrest (Figures 6G and 6J). These results suggest that SENP1 promotes STC1 expression by driving the SUMOylation of HIF-1α, thereby upregulating the expression of CCNE1 and promoting the viability and cell-cycle progression of Wilms tumor cells.

Silencing of SENP1 downregulated CCNE1 to inhibit the *in vivo* tumorigenesis of Wilms tumor cells

Finally, in order to study the effect of SENP1 on the *in vivo* tumorigenesis of Wilms tumor cells, we constructed WiT49 cell lines stably transfected with lentiviral vectors carrying sh-NC, sh-SENP1, sh-CCNE1, sh-SENP1 + oe-NC, and sh-SENP1 + oe-CCNE1 and then inoculated them subcutaneously into nude mice. Compared with sh-SENP1 alone, the tumor size and weight of sh-SENP1 + oe-CCNE1 transduction were increased (Figure 7A). Immunohistochemical results showed that the expression of CCNE1 in tumor tissues of nude mice transduced with sh-SENP1 and sh-CCNE1 was appreciably diminished. Compared with sh-SENP1 alone, the expression of CCNE1 in the presence of sh-SENP1 + oe-CCNE1 was appreciably increased (Figure 7B). Western blot results showed that the expression of HIF-1α, STC1, and CCNE1 in response to sh-SENP1 was appreciably diminished, and that of CCNE1 in response to sh-CCNE1 was appreciably diminished; relative to sh-SENP1 alone, the expression of CCNE1 in response to sh-SENP1 + oe-CCNE1 was appreciably increased (Figure 7C). Moreover, the expression of Ki67 and PCNA in tumor tissues of nude mice in response to sh-SENP1 combined with sh-CCNE1 was appreciably diminished. Compared with sh-SENP1 alone, the expression of Ki67 and PCNA in the presence of sh-SENP1 + oe-CCNE1 was

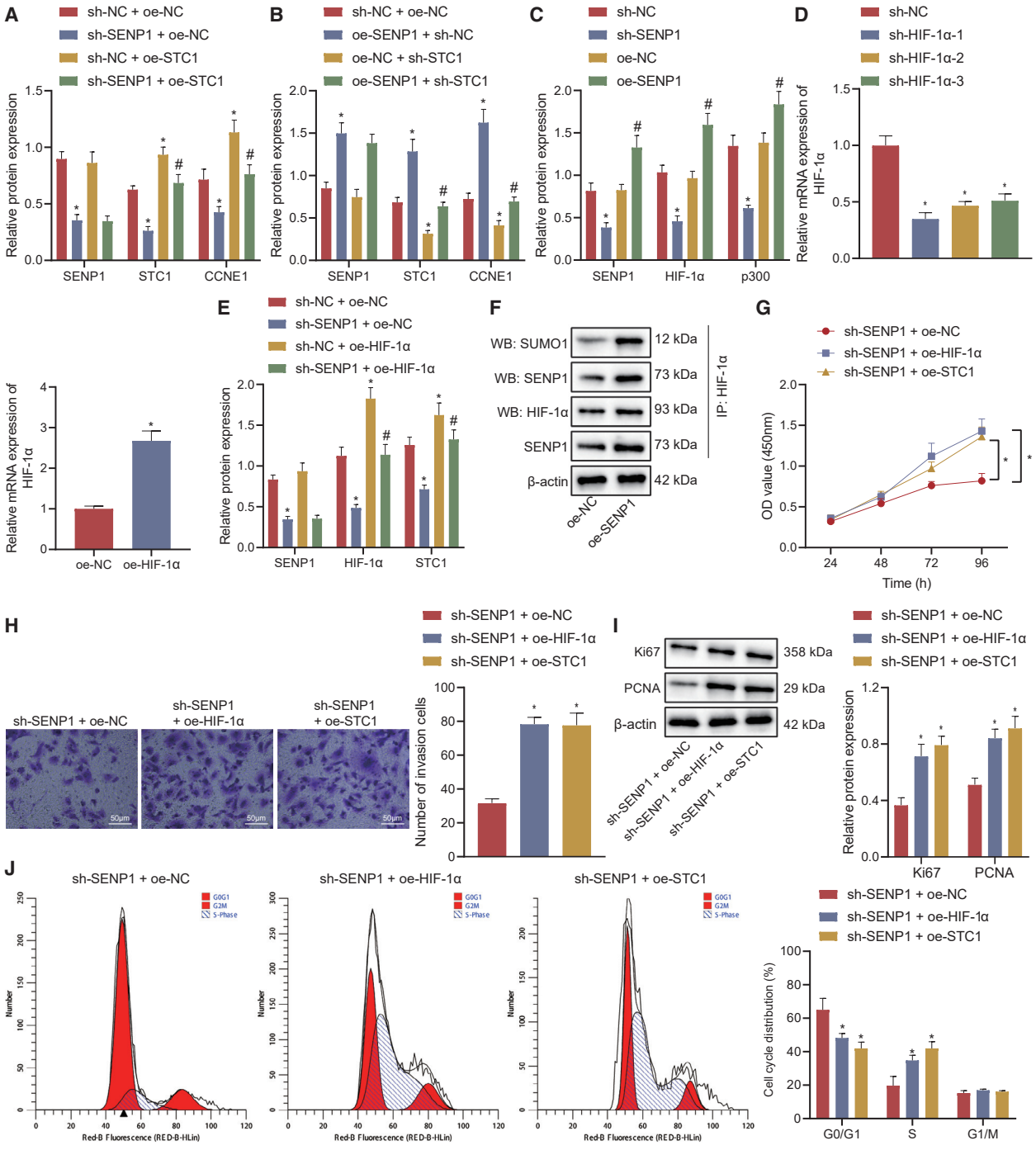

Figure 6. SENP1 promotes viability and cell-cycle progression of Wilms tumor cells by activating HIF1α/STC1/CCNE1 axis

(A) Western blot was used to detect the expression of SENP1, STC1, and CCNE1. *p < 0.05 versus the sh-NC + oe-NC group; #p < 0.05 versus the sh-SENP1 + oe-NC group. (B) Western blot was used to detect the expression of SENP1, STC1, and CCNE1. *p < 0.05 versus the sh-NC + oe-NC group; #p < 0.05 versus the oe-SENP1 + sh-NC group. (C) Western blot was used to detect the expression of SENP1, HIF-1α, and p300 in WiT49 cells after overexpression or silencing SENP1. *p < 0.05 versus the sh-NC group; #p < 0.05 versus the oe-NC group. (D) The expression of HIF-1α in WiT49 cells after silencing or overexpression of HIF-1 α was assayed by qRT-PCR. *p < 0.05 versus the sh-NC or oe-NC group. (E) The protein expression of SENP1, HIF-1α, and STC1 was assayed by western blot. *p < 0.05 versus the sh-NC + oe-NC group; #p < 0.05 versus the sh-SENP1 + oe-NC group. (F) The deSUMOylation of HIF-1α after overexpression of SENP1 was detected by IP assay. (G) Cell viability was detected by CCK-8 assay. (H) Cell invasion was detected by the Transwell assay. (I) Western blot was used to determine the expression of PCNA and Ki67. (J) Cell-cycle distribution was assayed by flow cytometry. (G–J) *p < 0.05 versus the sh-SENP1 + oe-NC group.

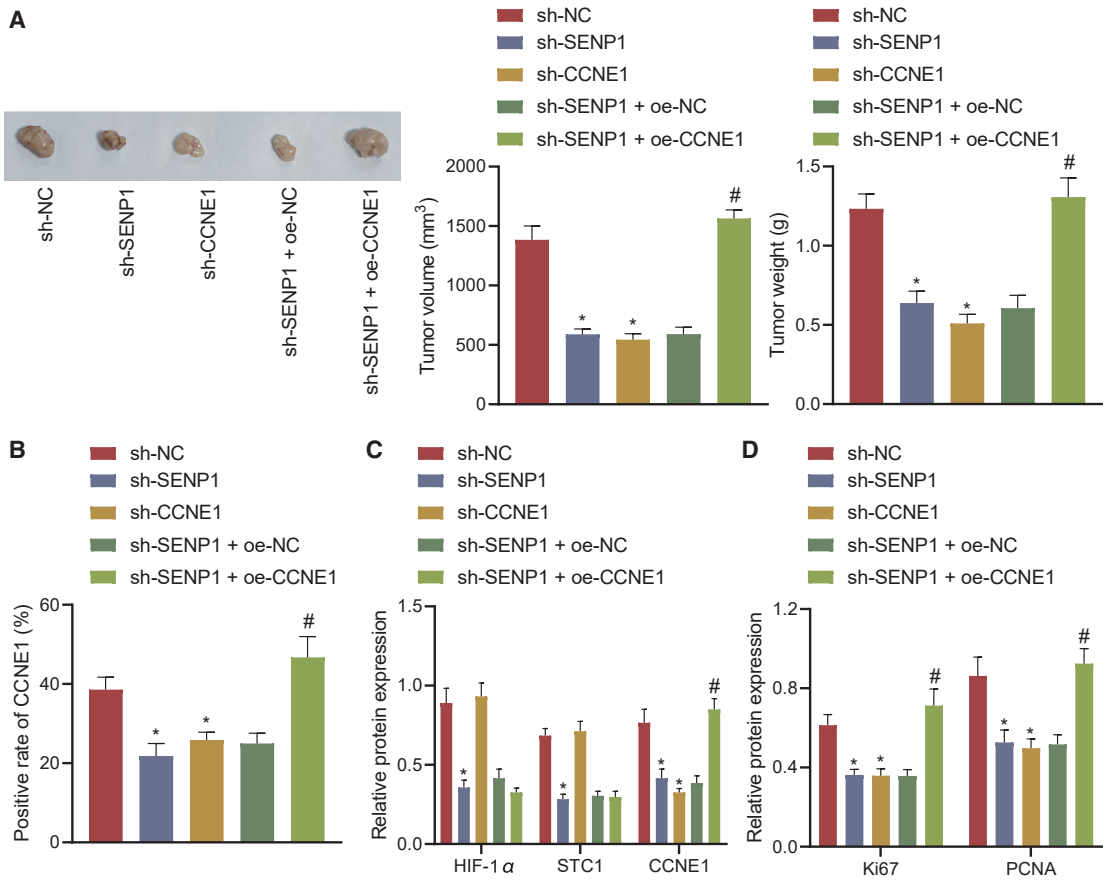

Figure 7. Silencing of SENP1 downregulates CCNE1 to inhibit the *in vivo* tumorigenesis of Wilms tumor cells

(A) The tumor volume and weight of nude mice in each group were counted. (B) The expression of CCNE1 in tumor tissue of nude mice in each group was assayed by immunohistochemical staining. (C) The expression of HIF-1α and STC1 in tumor tissue of nude mice in each group was assayed by western blot. (D) The protein expression of Ki67 and PCNA in tumor tissue of nude mice in each group was assayed by western blot. *p < 0.05 versus the sh-NC group. #p < 0.05 versus the sh-SENP1 + oe-NC group.

notably increased (Figure 7D). These results indicate that silencing of SENP1 downregulates the expression of CCNE1 and inhibits the tumorigenesis of Wilms tumor cells *in vivo*.

DISCUSSION

Wilms tumor takes up more than 90% of malignant renal neoplasms in children.[19] In the current study, we explored the regulatory mechanism of SENP1 in Wilms tumor and found that SENP1 promotes the progression of Wilms tumor through mediation of the HIF-1α/STC1/CCNE1 axis.

In the first place, our study demonstrated that SENP1 was highly expressed in Wilms tumor tissues as well as cells and that silencing of SENP1 could inhibit the viability and cell-cycle entry of Wilms tumor cells. To our acknowledge, SENP1 has been reported to be involved in multiple cancer types. For instance, restored SENP1 expression could aid in promoting renal cell carcinoma cell proliferation.[20] SENP1 was unveiled to be a risk factor for dissatisfactory prognosis of patients with non-small cell lung cancer.[21] Moreover, SENP1 could lead to enhancement of progression and metastasis of prostate cancer.[22] Furthermore, the current study revealed that SENP1 could trigger SUMOylation of HIF-1α in Wilms tumor, thereby upregulating HIF-1α. In consistency with our finding, an increasing number of studies have unveiled the regulatory relationship between SENP1 and HIF-1α. Interestingly, SENP1 could contribute to upregulation of HIF-1α expression under hypoxia in human osteosarcoma cells.[23] Notably, the implication of HIF-1α has been previously reported. Downregulation of HIF-1α using RNA interference was found to suppress the *in vitro* growth of SK-NEP-1 Wilms tumor cells, while inhibiting *in vivo* tumorigenesis and angiogenesis.[24]

Our mechanistic study also showed that HIF-1α could promote the expression of STC1, which contributed to upregulated STC1 in Wilms tumor, thereby leading to increased CCNE1 expression. Importantly, a previous study demonstrated upregulation of HIF-1α in Wilms tumor.[14] Of note, mounting evidence has highlighted the interaction between HIF-1α and STC1 in different diseases. As previously reported, a close correlation between STC1 mRNA

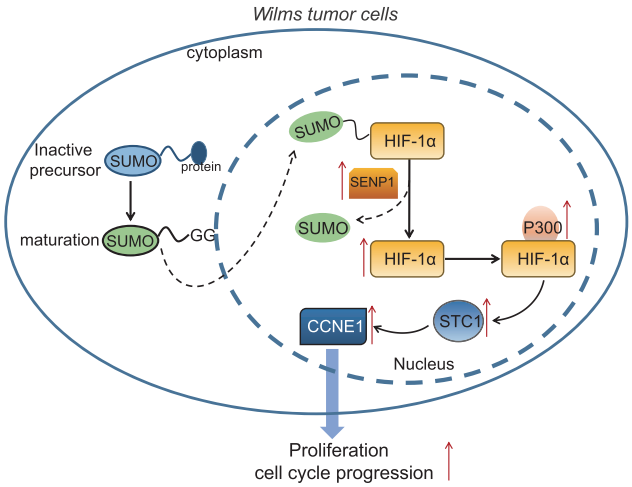

Figure 8. The molecular mechanism regarding the role of SENP1 in Wilms tumor

SENP1 promotes the expression of STC1 by increasing the SUMOylation of HIF-1α, upregulating the expression of CCNE1, which promotes the proliferation and cell-cycle progression of Wilms tumor cells.

expression and HIF-1α was observed in clear cell renal cell carcinoma cell lines, and the positive association between the two was also demonstrated in clinical samples, suggesting that HIF-1α is capable of regulating STC1 expression.[15] It was also demonstrated that HIF-1 plays a crucial role in the development of corpus luteum, with the involvement of STC1 regulation.[25] In addition, STC1 was found to be stimulated by HIF in alveolar epithelial cells in a rat model.[26] In fact, there is a paucity of reports regarding the regulation between STC1 and CCNE1 in disease. In the current study, our western blot assay identified that STC1 could positively regulate CCNE1 in Wilms tumor. Intriguingly, CCNE1 regulated by WWOX could participate in the regulation of Wilms tumor.[18] It was revealed that CCNE1 could be downregulated by WT1, which was demonstrated as a suppressor gene in Wilms tumor.[27]

Viewed from the results obtained in the current study, it is safe to conclude that SENP1 elevates STC1 expression by driving the SUMOylation of HIF-1α, thereby upregulating the expression of CCNE1, which promotes the viability, invasion, cell-cycle progression, and *in vivo* tumorigenesis of Wilms tumor cells (Figure 8). This finding may provide a novel direction for treatment of Wilms tumor. However, further exploration is still warranted to study the clinical feasibility.

MATERIALS AND METHODS

Ethical approval

The present study was conducted under the approval of the Ethics Committee of Guangzhou Women and Children's Medical Center, Guangzhou Medical University. The guardians of all of the participating patients signed informed consent. (A total of 32 consents were obtained.) The animal experiments strictly obeyed the guidelines for the care and use of laboratory animals issued by the US National Institutes of Health.

Bioinformatics analysis

A Wilms tumor-related microarray dataset GEO: GSE11151 [28] (3 normal samples and 3 tumor samples) was retrieved from the GEO database (https://www.ncbi.nlm.nih.gov/geo/). Relative to normal samples, differential analysis was performed using the "limma" package (version [v.]3.6.1) in R language (https://www.r-project.org/; v.3.6.1). False discovery rate (FDR) was used to correct differential p values, and DEGs in Wilms tumor were screened out with $|\log\text{FoldChange}| > 1$ and FDR < 0.05 as the threshold. The "clusterprofiler" package (v.3.0.4) in R language was employed for KEGG pathway enrichment analysis on DEGs. DEGs during cell cycle were labeled by "Pathview." Interaction analysis on DEGs during cell cycle was performed using the STRING database (https://string-db.org/; v.11.0). Then, an interaction network was plotted using Cytoscape software (https://cytoscape.org/; v.3.7.1), and degree values were calculated with interaction score $\geq$ 0.4 set as a threshold.

Clinical sample collection

From June 2015 to June 2017, 32 patients with Wilms tumor were selected, including 18 males and 14 females. The age distribution was 2−9 years old, with an average age of 4.34 ± 1.72 years. None of these patients received anti-tumor treatment before operation. All patients were detected on the basis of preoperative imaging and could be treated with radical nephrectomy. Patients with distant metastasis and cachexia were excluded in the study. The tumor tissues of 32 patients were included in the experimental group, and the control group indicated the paracancerous tissues. The paracancerous tissues and tumor tissues of each patient were taken as a group for subsequent experiment. The patients were followed up from the end of surgery for 24 months. The Kaplan-Meier method was performed to analyze the relationship between SENP1 and CCNE1 expression and OS and DFS of the patients.

Cell line screening, culture, and transfection

Wilms tumor cell lines, WiT49 cells (purchased from BLUEFBIO Biotechnology, Shanghai, China) and SK-NEP-1 cells (purchased from the Cell Bank of the Chinese Academy of Sciences, Shanghai, China), were included in this study. The 293T cells from normal renal tissue (purchased from ATCC, Manassas, VA, USA) were used as control. They were cultured in Dulbecco's modified Eagle medium (DMEM) containing 10% fetal bovine serum (FBS; Gibco, Carlsbad, CA, USA), 10 μg/mL streptomycin, and 100 U/mL penicillin (Gibco) at 37°C in a 5% CO_2 incubator (Thermo Fisher Scientific, Waltham, MA, USA). Cells in logarithmic phase were trypsinized, and the cells were seeded into a 6-well plate, 1×10^5 cells per well. After 24 h of conventional culture, the cells were transfected according to the instructions of Lipofectamine 2000 (Invitrogen, Carlsbad, CA, USA) when the confluence reached about 75%.

Transfection groups are as follows: sh-NC group (Wilms tumor cells transfected with the 5′-GGGUGAACUCACUGAGAA-3′ sequence), sh-SENP1-1 group (Wilms tumor cells transfected with the 5′-CACAGGAAGCGAGUGUGUGUGGU-3′ sequence), sh-SENP1-2 group (Wilms tumor cells transfected with the 5′-GAGGTAUCUTTUCGUUAUC-3′ sequence), and sh-SENP1-3 group (Wilms tumor

cells transfected with the 5′-GAUCUUGAUCCAUGA-3′ sequence). After 48 h of transfection, the silencing efficiency of sh-SENP1 was assessed by qRT-PCR. Additionally, the oe-SENP1 (Wilms tumor cells transfected with oe-SENP1), vector-NC (pGIPZ; Wilms tumor cells transfected with control plasmid), sh-CCNE1-1, sh-CCNE1-2, sh-CCNE1-3, sh-HIF-1α-1, sh-HIF-1α-2, sh-HIF-1α-3, oe-CCNE1, and oe-STC1 were purchased from GenePharma (Shanghai, China). The concentration of plasmid was 50 ng/mL.

CCK-8 assay

After 48 h of transfection, the cells were detached and resuspended, and the cell concentration was adjusted to 1×10^5 cells/mL. The cells were seeded into 96-well plates at 100 μL/well and cultured overnight. The cells were treated according to the instructions of the CCK-8 Kit (Beyotime, Shanghai, China). The cell viability was detected by CCK-8 assay at 24 h, 48 h, 72 h, and 96 h after inoculation. Each time, 10 μL CCK-8 detection solution was added and incubated in the incubator for 4 h. The absorbance at 450 nm was detected by a plate reader (Thermo Scientific Multiskan FC; Thermo Fisher Scientific), and the growth curve was drawn.

Transwell invasion assay

Matrigel chambers (BD Biosciences, Franklin Lakes, NJ, USA) were incubated on the upper surface of the bottom membrane of Transwell chambers at 37°C for 30 min to make Matrigel polymerize into gel, and then the basement membrane was hydrated before use. The cells were cultured in serum-free medium for 12 h, harvested, and resuspended in serum-free medium (1×10^5 cells/mL). The medium containing 10% FBS was added in the lower chamber, and 100 μL cell suspension was added into the Transwell chamber. After incubation at 37°C for 24 h, the cells that did not invade the surface of the Matrigel membrane were gently removed with cotton swabs, fixed with 100% methanol, and stained with 1% toluidine blue (Sigma-Aldrich Chemical, St. Louis, MO, USA). The stained, invasive cells were observed under an inverted light microscope (Carl Zeiss MicroImaging, Thornwood, NY, USA). Five areas were randomly selected for manual counting.

Flow cytometry

Cells in the logarithmic growth phase were seeded into a 6-well plate (about 5×10^4 cells/well). After cell-adherent growth, the former culture medium was removed from the culture dish, followed by addition of sterile normal saline, digestion, and collection of the single-cell suspension. It was fixed overnight with 20 mL of 75% alcohol precooled at 75°C, added with propidium iodide (PI) and RNase, and incubated at 37°C for 30 min in dark. The cell-cycle distribution in G0/G1, S, and G2/M phases was assayed by flow cytometry.

RNA IP (RIP) assay

Cells were lysed with ice-cold IP lysis buffer containing phosphatase-protease inhibitor cocktails (Beyotime Biotechnology, Shanghai, China). After centrifugation at 12,000 rpm, the protein supernatant was incubated with primary antibody at 4°C overnight. The protein-antibody complex was pulled down with Protein A/G PLUS-Agarose Beads (Santa Cruz, Santa Cruz, CA, USA). Those beads were eluted with IP lysis buffer 4 times. Next, 45 μL 2× loading buffer was added to the agarose beads, 10 μL 5× loading buffer was added to the input, followed by boiling for 10 min. The IP protein was eluted for western blot analysis.

qRT-PCR

TRIzol reagent (15596026; Invitrogen) was employed to extract total RNA. According to the instructions of the PrimeScript RT Reagent Kit (RR047A; Takara, Otsu, Shiga, Japan), 5 μg RNA was reversely transcribed into complementary DNA (cDNA). The synthesized 10-ng cDNA was detected using Fast SYBR Green PCR kits (Applied Biosystems [ABI], Carlsbad, CA, USA) in an ABI Prism 7300 RT-PCR system (ABI). Three replicated wells were set for each group. The relative expression levels of SENP1 and CCNE1 were analyzed by the $2^{-\Delta\Delta CT}$ method with β-actin as an internal reference. The primer design is shown in Table S1.

Western blot analysis

The cultured cells were collected by trypsin digestion and lysed with enhanced radioimmunoprecipitation assay lysis buffer containing a protease inhibitor (Boster, Wuhan, Hubei, China); then the protein concentration was determined by a bicinchoninic acid (BCA) protein quantitative kit (Boster). The protein was separated by 10% sodium dodecyl sulfate polyacrylamide gel electrophoresis and then transferred to a polyvinylidene fluoride membrane. Subsequently, the membrane was sealed with 5% bovine serum albumin at room temperature for 2 h to block the nonspecific binding. Diluted primary antibodies (SENP1: ab225887; CCNE1: ab71535; STC1: ab229477; HIF-1α: ab51608; p300: ab10485; rabbit antibody PCNA: ab18197; rabbit antibody Ki67: ab16667; rabbit antibody β-actin: ab8227, 1:500; Abcam, Cambridge, MA, USA) were added to the membrane, respectively, for overnight incubation at 4°C. Horseradish peroxidase (HRP)-labeled goat anti-rabbit antibody (ab205719; 1:2,000; Abcam) was employed to incubate the membrane at room temperature for 1 h. Enhanced chemiluminescence working solution (Millipore) was employed to incubate the membrane at room temperature for 1 min, which was then sealed and exposed to X-ray for 5–10 min, followed by color development and fixation. ImageJ analysis software was employed to quantify the gray scale of each band in western blot image, and β-actin was used as an internal reference.

Tumor formation in nude mice

Thirty healthy nude mice (aged 6–8 weeks) were acclimated for 1 week (specific pathogen free; humidity: 60%–65%; temperature: 22°C–25°C; 12/12 h light-dark cycle), with free access to food and water. The health status of nude mice was observed before the experiment. WiT49 cells were stably transduced with sh-NC, sh-SENP1, sh-CCNE1, sh-SENP1 + oe-NC, and sh-SENP1 + oe-CCNE1. The nude mice were randomly divided into 5 groups, with 6 mice in each group. During the feeding process, 100 μL of stably transduced cells was subcutaneously injected into the armpit of nude mice. After 6 weeks of feeding, the nude mice were euthanized, following which, the tumor size was measured. The tumors were resected, weighed, and collected for subsequent detections.

Immunohistochemical staining

Following antigen retrieval, the samples were treated with normal goat serum blocking solution (C-0005; Shanghai Haoran Biotechnology, Shanghai, China) for 20 min at room temperature. The primary rabbit antibody against CCNE1 (ab33911, 1:200; Abcam) was added for overnight incubation at 4°C, followed by incubation with goat anti-rabbit immunoglobulin G (IgG; ab150077, 1:1,000; Abcam) at 37°C for 20 min. Sections were subjected to HRP-labeled streptavidin working solution (0343-10000U; Imunbio, Beijing, China) at 37°C for 20 min. Following diaminobenzidine (ST033; Whiga, Guangdong, China) developing, sections were re-stained by hematoxylin (PT001; Shanghai Bogoo Technology, Shanghai, China), treated with 1% ammonia water to revert to blue, dehydrated, and mounted. Five high-power fields were randomly selected from each section, with 100 cells counted in each field under microscopy.

Statistical analysis

All of the data in this study were processed with SPSS 21.0 statistical software (IBM, Armonk, NY, USA). The measurement data were expressed by mean ± standard deviation from three independent experiments. Paired t test was employed to compare data between cancer tissues and adjacent normal tissues. Data between two groups were compared by unpaired t test. Data among multiple groups were compared by one-way analysis of variance (ANOVA) and those among multiple groups at different time points by repeated measures of ANOVA, followed by Tukey's post hoc test. The Kaplan-Meier method was employed to calculate the survival rate. The log rank test was used for univariate analysis. Pearson's correlation analysis was employed to analyze the correlation between observed indexes. $p < 0.05$ indicated a statistically significant difference.

SUPPLEMENTAL INFORMATION

Supplemental information can be found online at https://doi.org/10.1016/j.omto.2021.07.007.

ACKNOWLEDGMENTS

We thank our colleagues for technical help and stimulating discussions. The datasets generated/analyzed during the current study are available. This work is supported by Guangzhou Institute of Pediatrics/Guangzhou Women and Children's Medical Center (GWCMC2020-4-009), Science and Technology Projects in Guangzhou (202102020097) and Natural Science Foundation of Guangdong Province, China (grant number [no.]: 2019A1515011178).

AUTHOR CONTRIBUTIONS

S.Z. and J.H. wrote the paper and designed the experiments. X.G. and J.Z. conducted the experiments. Y.C. and S.L. analyzed the data. W.J. collected and provided the sample for this study. All authors have read and approved the final submitted manuscript.

DECLARATION OF INTERESTS

The authors declare no competing interests.

REFERENCES

1. Sudour-Bonnange, H., Coulomb-Lherminé, A., Fantoni, J.C., Escande, A., Brisse, H.J., Thebaud, E., and Verschuur, A. (2021). Standard of care for adult Wilms tumor? From adult urologist to pediatric oncologist. A retrospective review. Bull. Cancer *108*, 177–186.

2. Dumba, M., Jawad, N., and McHugh, K. (2015). Neuroblastoma and nephroblastoma: a radiological review. Cancer Imaging *15*, 5.

3. Brisse, H.J., de la Monneraye, Y., Cardoen, L., and Schleiermacher, G. (2020). From Wilms to kidney tumors: which ones require a biopsy? Pediatr. Radiol. *50*, 1049–1051.

4. Treger, T.D., Chowdhury, T., Pritchard-Jones, K., and Behjati, S. (2019). The genetic changes of Wilms tumour. Nat. Rev. Nephrol. *15*, 240–251.

5. Vujanić, G.M., Gessler, M., Ooms, A.H.A.G., Collini, P., Coulomb-l'Hermine, A., D'Hooghe, E., de Krijger, R.R., Perotti, D., Pritchard-Jones, K., Vokuhl, C., et al.; International Society of Paediatric Oncology–Renal Tumour Study Group (SIOP–RTSG) (2018). The UMBRELLA SIOP-RTSG 2016 Wilms tumour pathology and molecular biology protocol. Nat. Rev. Urol. *15*, 693–701.

6. Chen, C.H., Namanja, A.T., and Chen, Y. (2014). Conformational flexibility and changes underlying activation of the SUMO-specific protease SENP1 by remote substrate binding. Nat. Commun. *5*, 4968.

7. Heo, K.S. (2019). Regulation of post-translational modification in breast cancer treatment. BMB Rep. *52*, 113–118.

8. Bouchard, D.M., and Matunis, M.J. (2019). A cellular and bioinformatics analysis of the SENP1 SUMO isopeptidase in pancreatic cancer. J. Gastrointest. Oncol. *10*, 821–830.

9. Tao, Y., Li, R., Shen, C., Li, J., Zhang, Q., Ma, Z., Wang, F., and Wang, Z. (2020). SENP1 is a crucial promotor for hepatocellular carcinoma through deSUMOylation of UBE2T. Aging (Albany NY) *12*, 1563–1576.

10. Zhou, G.Q., Han, F., Shi, Z.L., Yu, L., Li, X.F., Yu, C., Shen, C.L., Wan, D.W., Zhu, X.G., Li, R., and He, S.B. (2018). miR-133a-3p Targets SUMO-Specific Protease 1 to Inhibit Cell Proliferation and Cell Cycle Progress in Colorectal Cancer. Oncol. Res. *26*, 795–800.

11. Ao, Q., Su, W., Guo, S., Cai, L., and Huang, L. (2015). SENP1 desensitizes hypoxic ovarian cancer cells to cisplatin by up-regulating HIF-1α. Sci. Rep. *5*, 16396.

12. Fraga, A., Ribeiro, R., Príncipe, P., Lobato, C., Pina, F., Maurício, J., Monteiro, C., Sousa, H., Calais da Silva, F., Lopes, C., and Medeiros, R. (2014). The HIF1A functional genetic polymorphism at locus +1772 associates with progression to metastatic prostate cancer and refractoriness to hormonal castration. Eur. J. Cancer *50*, 359–365.

13. Maturu, P., Jones, D., Ruteshouser, E.C., Hu, Q., Reynolds, J.M., Hicks, J., Putluri, N., Ekmekcioglu, S., Grimm, E.A., Dong, C., and Overwijk, W.W. (2017). Role of Cyclooxygenase-2 Pathway in Creating an Immunosuppressive Microenvironment and in Initiation and Progression of Wilms' Tumor. Neoplasia *19*, 237–249.

14. Dungwa, J.V., Hunt, L.P., and Ramani, P. (2011). Overexpression of carbonic anhydrase and HIF-1α in Wilms tumours. BMC Cancer *11*, 390.

15. Ma, X., Gu, L., Li, H., Gao, Y., Li, X., Shen, D., Gong, H., Li, S., Niu, S., Zhang, Y., et al. (2015). Hypoxia-induced overexpression of stanniocalcin-1 is associated with the metastasis of early stage clear cell renal cell carcinoma. J. Transl. Med. *13*, 56.

16. Chang, A.C., Doherty, J., Huschtscha, L.I., Redvers, R., Restall, C., Reddel, R.R., and Anderson, R.L. (2015). STC1 expression is associated with tumor growth and metastasis in breast cancer. Clin. Exp. Metastasis *32*, 15–27.

17. Zubillaga-Guerrero, M.I., Alarcón-Romero, Ldel.C., Illades-Aguiar, B., Flores-Alfaro, E., Bermúdez-Morales, V.H., Deas, J., and Peralta-Zaragoza, O. (2015). MicroRNA miR-16-1 regulates CCNE1 (cyclin E1) gene expression in human cervical cancer cells. Int. J. Clin. Exp. Med. *8*, 15999–16006.

18. Płuciennik, E., Nowakowska, M., Wujcicka, W.I., Sitkiewicz, A., Kazanowska, B., Zielińska, E., and Bednarek, A.K. (2012). Genetic alterations of WWOX in Wilms' tumor are involved in its carcinogenesis. Oncol. Rep. *28*, 1417–1422.

19. Cunningham, M.E., Klug, T.D., Nuchtern, J.G., Chintagumpala, M.M., Venkatramani, R., Lubega, J., and Naik-Mathuria, B.J. (2020). Global Disparities in Wilms Tumor. J. Surg. Res. *247*, 34–51.

20. Jiao, D., Wu, M., Ji, L., Liu, F., and Liu, Y. (2018). MicroRNA-186 Suppresses Cell Proliferation and Metastasis Through Targeting Sentrin-Specific Protease 1 in Renal Cell Carcinoma. Oncol. Res. *26*, 249–259.

21. Liu, K., Zhang, J., and Wang, H. (2018). Small ubiquitin-like modifier/sentrin-specific peptidase 1 associates with chemotherapy and is a risk factor for poor prognosis of non-small cell lung cancer. J. Clin. Lab. Anal. *32*, e22611.

22. Wang, Q., Xia, N., Li, T., Xu, Y., Zou, Y., Zuo, Y., Fan, Q., Bawa-Khalfe, T., Yeh, E.T., and Cheng, J. (2013). SUMO-specific protease 1 promotes prostate cancer progression and metastasis. Oncogene *32*, 2493–2498.

23. Wang, X., Liang, X., Liang, H., and Wang, B. (2018). SENP1/HIF-1α feedback loop modulates hypoxia-induced cell proliferation, invasion, and EMT in human osteosarcoma cells. J. Cell. Biochem. *119*, 1819–1826.

24. Shi, B., Li, Y., Wang, X., Yang, Y., Li, D., Liu, X., and Yang, X. (2016). Silencing of hypoxia inducible factor-1α by RNA interference inhibits growth of SK-NEP-1 Wilms tumour cells in vitro, and suppresses tumourigenesis and angiogenesis in vivo. Clin. Exp. Pharmacol. Physiol. *43*, 626–633.

25. Meidan, R., Klipper, E., Zalman, Y., and Yalu, R. (2013). The role of hypoxia-induced genes in ovarian angiogenesis. Reprod. Fertil. Dev. *25*, 343–350.

26. Ito, Y., Zemans, R., Correll, K., Yang, I.V., Ahmad, A., Gao, B., and Mason, R.J. (2014). Stanniocalcin-1 is induced by hypoxia inducible factor in rat alveolar epithelial cells. Biochem. Biophys. Res. Commun. *452*, 1091–1097.

27. Loeb, D.M., Korz, D., Katsnelson, M., Burwell, E.A., Friedman, A.D., and Sukumar, S. (2002). Cyclin E is a target of WT1 transcriptional repression. J. Biol. Chem. *277*, 19627–19632.

28. Yusenko, M.V., Kuiper, R.P., Boethe, T., Ljungberg, B., van Kessel, A.G., and Kovacs, G. (2009). High-resolution DNA copy number and gene expression analyses distinguish chromophobe renal cell carcinomas and renal oncocytomas. BMC Cancer *9*, 152.